

# Wilson Fermion Determinant in Lattice QCD

Keitaro Nagata

*Department of Physics, The University of Tokyo,  
Bunkyo-ku, Tokyo 113-0033 JAPAN*

Atsushi Nakamura

*Research Institute for Information Science and Education,  
Hiroshima University,  
Higashi-Hiroshima 739-8527 JAPAN*

(Dated: February 5, 2022)

We present a formula for reducing the rank of Wilson fermions from  $4N_c N_x N_y N_z N_t$  to  $4N_c N_x N_y N_z$  keeping the value of its determinant. We analyse eigenvalues of a reduced matrix and coefficients  $C_n$  in the fugacity expansion of the fermion determinant  $\sum_n C_n (\exp(\mu/T))^n$ , which play an important role in the canonical formulation, using lattice QCD configurations on a  $4^4$  lattice. Numerically,  $\log |C_n|$  varies as  $N_x N_y N_z$ , and goes easily over the standard numerical range; We give a simple cure for that. The phase of  $C_n$  correlates with the distribution of the Polyakov loop in the complex plain. These results lay the groundwork for future finite density calculations in lattice QCD.

PACS numbers: 12.38.Lg, 12.38.Mh, 21.65.Qr

## I. INTRODUCTION

QCD at finite temperature and density has been one of the most attracting subjects in physics. Many phenomenological models predict that the QCD phase diagram is expected to have a very rich structure, and thoroughgoing analyses of heavy ion data have been made to show that we are sweeping finite temperature and density regions. See Ref. [1].

First-principle calculations based on QCD are now highly called. If such calculations would be at our hand, their outcomes are also very valuable for many research fields: high energy heavy ion collisions, the high density interior of neutron stars and the last stages of the star evolution. Needless to say, the inside of nucleus is also a baryon rich environment, and lots of contributions to nuclear physics could be expected.

Unfortunately, the first principle lattice QCD simulation suffers from the sign problem. Nevertheless, there have been many progresses such as the reweighting method[2], the imaginary chemical potential[3, 4] and the canonical formulation[5, 6]; now some light is shed on the QCD phase diagram.

Most of lattice QCD studies with non-zero density were done with the use of staggered fermions. It is desirable to study lattice QCD with Wilson fermions because it is free from the fourth-root problem. At zero density, thanks to several algorithm developments, lattice QCD simulations with Wilson fermions are now possible even on the physical quark masses.

In case of the lattice QCD simulations with finite chemical potential  $\mu$ , often we must handle the fermion determinant  $\det \Delta(\mu)$ , directly. For example, the reweighting method requires a ratio of two determinants,

$$\frac{\det \Delta(\mu')}{\det \Delta(\mu)}. \quad (1)$$

The density of state method needs the phase information[7]. The canonical formulation needs the Fourier transformation of the fermion determinant

$$\det \Delta_n = \frac{1}{2\pi} \int d\left(\frac{\mu_I}{T}\right) e^{-in\mu_I/T} \det \Delta(\mu_I), \quad (2)$$

with the quark number  $n$  and the imaginary chemical potential  $\mu_I$ . In these approaches, the heaviest part of the numerical calculations is the evaluation of the determinant. An efficient way of the determinant evaluation is highly desirable. It is very useful if we can transform the fermion matrix  $\Delta$  into a compressed one whose rank is less than the original one, and yet it gives the same value of the determinant, since the numerical cost to evaluate a determinant is usually proportional to the third power of the matrix rank.

Such a transformation was found for the staggered fermion by Gibbs [8] and Hasenfratz and Toussaint [9], and used in finite density simulations, e.g. [10–13]. Their method has also an advantage in the canonical formulation. With the reduction method, the fermion determinant is expressed in powers of fugacity,

$$\det \Delta(\mu) = \sum_n C_n \left(e^{\mu/T}\right)^n. \quad (3)$$

If we obtain the coefficients  $C_n$ , the Fourier transformation in the canonical formulation is easily carried out.

A reduction method for Wilson fermions has not been established yet. It is unfeasible to apply the method for staggered fermions in [8, 9] to Wilson fermions in a naive way because of singular parts contained in the Wilson fermion matrix. Expansions based on the trace-log formula have been proposed for the Wilson fermion determinant [14–21]. An efficient method to calculate exactly the Wilson fermion determinant is valuable for finite density simulations with Wilson fermions.

The purpose of the present work is to construct a reduction method for Wilson fermions. In Ref. [22], Borici derived a reduction method that can be applied to Wilson fermions, and tested it using a Schwinger model (QED2) with staggered fermions. We develop further the method of [22] and derive a reduction formula, which rearranges the Wilson fermion determinant in powers of fugacity and reduces the numerical cost.

Similar to the method in [8, 9], the Wilson fermion matrix is expressed in a time-plane block matrix form. Projection operators contained in the Wilson fermion matrix make it possible to transform forward and backward hopping parts separately. Owing to the property of the projection operators, the Wilson fermion matrix is transformed so that the determinant in the time-plane block form can be carried out analytically. The determinant of the Wilson fermion is then reduced into that of a reduced matrix, whose size is smaller than the original one. The problem results in the diagonalization of the reduced matrix instead of the original matrix. Solving the eigenvalue problem for the reduced matrix, the Wilson fermion determinant is expressed in powers of fugacity.

This paper is organized as follow. In the next section, we show the reduction method for the Wilson fermions. In section III, as an illustration, we perform numerical simulations on a small  $4^4$  lattice and calculate the Wilson fermion determinant using the reduction method. We discuss the properties of the coefficients of the fugacity expansion. The results are not to be regarded as physical, due to the small lattice size, but lay the groundwork for future realistic calculations. The final section is devoted to a summary. In the appendix, we give (1) the detail of the calculation of the determinant of a permutation matrix  $P$  used in the reduction formula, (2) a simple numerical trick to evaluate the fugacity expansion coefficients, and (3) a possible alternative formulation.

## II. FRAMEWORK

### A. Structure of Fermion Matrix

We employ the Wilson fermions defined by

$$\begin{aligned}
\Delta(x, x') = & \delta_{x, x'} - \kappa \sum_{i=1}^3 \left\{ (r - \gamma_i) U_i(x) \delta_{x', x+\hat{i}} + (r + \gamma_i) U_i^\dagger(x') \delta_{x', x-\hat{i}} \right\} \\
& - \kappa \left\{ e^{+\mu} (r - \gamma_4) U_4(x) \delta_{x', x+\hat{4}} + e^{-\mu} (r + \gamma_4) U_4^\dagger(x') \delta_{x', x-\hat{4}} \right\} \\
& + S_{Clover}, \\
S_{Clover} = & - \delta_{x, x'} C_{SW} \kappa \sum_{\mu \leq \nu} \sigma_{\mu\nu} F_{\mu\nu}.
\end{aligned} \tag{4}$$

where  $r$ ,  $\kappa$  and  $\mu$  are the Wilson term, hopping parameter and chemical potential, respectively. We include the clover term with the coefficient  $C_{SW}$ . For later convenience, we divide the quark matrix into three terms according to their time dependence

$$\Delta = B - 2z^{-1}\kappa r_- V - 2z\kappa r_+ V^\dagger. \tag{5}$$

Here  $r_\pm = (r \pm \gamma_4)/2$  and  $z = e^{-\mu}$ , and

$$\begin{aligned}
B(x, x') \equiv & \delta_{x, x'} - \kappa \sum_{i=1}^3 \left\{ (r - \gamma_i) U_i(x) \delta_{x', x+\hat{i}} + (r + \gamma_i) U_i^\dagger(x') \delta_{x', x-\hat{i}} \right\} \\
& + S_{Clover},
\end{aligned} \tag{6}$$

$$V(x, x') \equiv U_4(x) \delta_{x', x+\hat{4}}, \tag{7}$$

$$V^\dagger(x, x') \equiv U_4^\dagger(x') \delta_{x', x-\hat{4}}. \tag{8}$$

They satisfy  $VV^\dagger = I$ . Note that  $r_\pm$  are projection operators in the case that  $r = 1$ . In a time-plane block matrix form,  $B$  and  $V$  are given by

$$B = \begin{array}{c} \begin{array}{cc} t'=1 & \dots & t'=N_t \end{array} \\ \begin{array}{c} t=1 \\ t=2 \\ t=3 \\ \vdots \\ \vdots \\ t=N_t \end{array} \end{array} \left( \begin{array}{c|c|c|c|c|c} B_1 & 0 & 0 & \dots & 0 & 0 \\ \hline 0 & B_2 & 0 & \dots & 0 & 0 \\ \hline 0 & 0 & B_3 & \dots & & \\ \hline \dots & \dots & \dots & \dots & \dots & \dots \\ \hline & & & \dots & 0 & 0 \\ \hline 0 & 0 & & \dots & 0 & B_{N_t-1} \\ \hline 0 & 0 & & \dots & 0 & B_{N_t} \end{array} \right). \tag{9}$$

$$V = \left( \begin{array}{c|c|c|c} 0 & U_4(t=1) & 0 & \dots & 0 \\ \hline 0 & 0 & U_4(t=2) & \dots & 0 \\ \hline 0 & 0 & 0 & \dots & \\ \dots & \dots & \dots & \dots & \dots \\ \hline & & \dots & U_4(t=N_t-2) & 0 \\ \hline 0 & 0 & \dots & 0 & U_4(t=N_t-1) \\ \hline -U_4(t=N_t) & 0 & \dots & 0 & 0 \end{array} \right).$$

### B. Reduction Formula for Wilson Fermions

Now, we derive a reduction formula for the Wilson fermions. A starting point is to define a matrix [22],

$$P = (c_a r_- + c_b r_+ V z^{-1}), \quad (10)$$

which is referred to as a permutation matrix [22]. The parameters  $c_a$  and  $c_b$  are arbitrary scalar except for zero, and may be set to one. We can use these parameters to check the following reduction formula numerically. Since  $r_{\pm}$  are singular, the matrix  $P$  must contain both of them; otherwise  $P$  is singular. It is straightforward to check  $\det(P) = (c_a c_b z^{-1})^{N/2}$ , where  $N = 4N_c N_x N_y N_z N_t$ . Multiplied by  $P$ , the quark matrix is transformed into

$$\Delta P = (c_a B r_- - 2c_b \kappa r_+) + (c_b B r_+ - 2c_a \kappa r_-) V z^{-1}. \quad (11)$$

In the time-plane block matrix form, the first and second terms of Eq. (11) are given by

$$(c_a B r_- - 2c_b \kappa r_+) = \begin{pmatrix} \alpha_1 & & & \\ & \alpha_2 & & \\ & & \ddots & \\ & & & \alpha_{N_t} \end{pmatrix}, \quad (12)$$

$$(c_b B r_+ - 2c_a \kappa r_-) V z^{-1} = \begin{pmatrix} 0 & \beta_1 z^{-1} & & & \\ & 0 & \beta_2 z^{-1} & & \\ & & 0 & \ddots & \\ & & & \ddots & \beta_{N_t-1} z^{-1} \\ -\beta_{N_t} z^{-1} & & & & 0 \end{pmatrix}. \quad (13)$$

The block-matrices are given by

$$\begin{aligned} \alpha_i &= \alpha^{ab, \mu\nu}(\vec{x}, \vec{y}, t_i) \\ &= c_a B^{ab, \mu\sigma}(\vec{x}, \vec{y}, t_i) r_-^{\sigma\nu} - 2c_b \kappa r_+^{\mu\nu} \delta^{ab} \delta(\vec{x} - \vec{y}), \end{aligned} \quad (14)$$

$$\begin{aligned} \beta_i &= \beta^{ab, \mu\nu}(\vec{x}, \vec{y}, t_i), \\ &= c_b B^{ac, \mu\sigma}(\vec{x}, \vec{y}, t_i) r_+^{\sigma\nu} U_4^{cb}(\vec{y}, t_i) - 2c_a \kappa r_-^{\mu\nu} \delta(\vec{x} - \vec{y}) U_4^{ab}(\vec{y}, t_i), \end{aligned} \quad (15)$$

where the dimensions of  $\alpha_i$  and  $\beta_i$  are given by  $N_{\text{red}} = N/N_t = 4N_x N_y N_z N_c$ . We factor out a negative sign caused by anti-periodic boundary conditions from the definition of  $\beta_{N_t}$ . Therefore the negative sign appears at the lower-left corner in Eq. (13). The two block-matrices have different meaning;  $\alpha_i$  contains only spatial hopping terms with a fixed time  $t = t_i$ , while  $\beta_i$  contains temporal hopping terms as well as spatial ones due to temporal link variables.

Combining Eqs. (12) and (13), we can carry out the determinant in the time-plane block matrix

$$\begin{aligned} \det \Delta P &= \begin{vmatrix} \alpha_1 & \beta_1 z^{-1} & & & \\ & \alpha_2 & \beta_2 z^{-1} & & \\ & & \alpha_3 & \ddots & \\ & & & \ddots & \beta_{N_t-1} z^{-1} \\ -\beta_{N_t} z^{-1} & & & & \alpha_{N_t} \end{vmatrix} \\ &= \left( \prod_{i=1}^{N_t} \det(\alpha_i) \right) \det(1 + z^{-N_t} Q), \end{aligned} \quad (16)$$

where  $Q = (\alpha_1^{-1} \beta_1) \cdots (\alpha_{N_t}^{-1} \beta_{N_t})$ , which we refer to as a reduced matrix. Substituting  $\det(P) = (c_a c_b z^{-1})^{N/2}$ , we obtain

$$\det \Delta = (c_a c_b)^{-N/2} z^{-N/2} \left( \prod_{i=1}^{N_t} \det(\alpha_i) \right) \det(z^{N_t} + Q). \quad (17)$$

Here, the rank of the matrices  $\alpha_i$  and  $Q$  is given by  $N_{\text{red}} = N/N_t$ , while that of the Wilson fermion is originally given by  $N$ . Thus the reduction formula makes the computation of the determinant  $1/N_t^3$  less time. Furthermore, the  $\mu$  dependent parts are separated from the hopping terms, and appear at the overall factor and the second determinant.

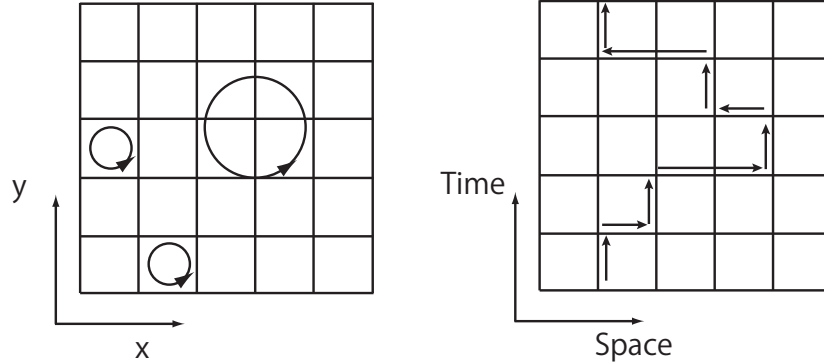


FIG. 1: The left panel depicts closed loops on a plane  $t = t_i$ , which contribute to  $\det \alpha_i$ , while the right one does paths of quarks from  $t = t_1$  to  $t = t_{N_t}$ , which contribute to the reduced matrix  $Q$ .

Equation (17) consists of sub-determinants:  $\prod \det(\alpha_i)$  and  $\det(z^{N_t} + Q)$ . As we have explained,  $\alpha_i$  describes spatial hopping terms at a time-slice with  $t_i$ . Hence,  $\det \alpha_i$  describes closed loops in a plane with a fixed time

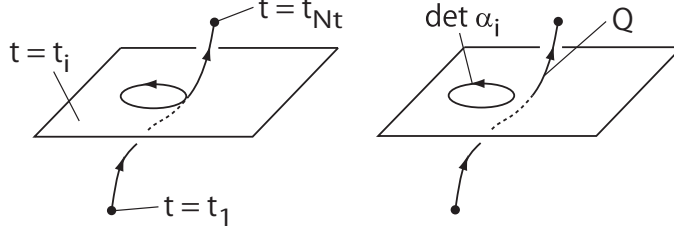


FIG. 2: Schematic figures for the reduction procedure.

$t = t_i$  (left panel in Fig. 1). On the other hand,  $\beta_i$  contains temporal hopping terms from  $t = t_i$  to  $t = t_{i+1}$ . The reduced matrix  $Q$  describes paths of the propagation of quarks from  $t = t_1$  to  $t = t_{N_t}$  (right panel in Fig. 1). Thus, the reduction formula separates closed loops at time-slices from paths of the propagation of quarks (Fig. 2).

Now, we solve an eigenvalue problem  $\det(Q - \lambda I) = 0$ . With the eigenvalues  $\lambda$ , the determinant of the reduced matrix is written as

$$\det(z^{N_t} + Q) = \prod_{n=1}^{N_{\text{red}}} (\lambda_n + z^{N_t}), \quad (18)$$

which is expanded in powers of  $z^{N_t}$ ,

$$\begin{aligned} z^{-N/2} \prod_{n=1}^{N_{\text{red}}} (\lambda_n + z^{N_t}) &= \sum_{n=-N_{\text{red}}/2}^{N_{\text{red}}/2} c_n (z^{N_t})^n \\ &= c_{-N_{\text{red}}/2} (z^{N_t})^{N_{\text{red}}/2} + \dots + c_0 + \dots + c_{N_{\text{red}}/2} (z^{N_t})^{-N_{\text{red}}/2}, \end{aligned} \quad (19)$$

where we replace  $c_n$  by  $c_{-n}$  to obtain the second line from the first one. This is an expansion with regard to (inverse) fugacity  $z^{N_t} = \exp(-\mu/T)$ . Equivalently, this can be interpreted as a winding number expansion, because  $z^{N_t}$  comes from closed loops that make a round the lattice in the time-direction. Note that the expansion Eq. (19) is exactly done and does not involve any approximation.

Finally, we obtain the reduced quark determinant

$$\det \Delta(\mu) = \sum_{n=-N_{\text{red}}/2}^{N_{\text{red}}/2} C_n (e^{\mu/T})^n, \quad (20)$$

Here,  $C_n = C c_n$  with  $C = (c_a c_b)^{-N/2} \left( \prod_{i=1}^{N_t} \det(\alpha_i) \right)$ .

The coefficients  $c_n$  have two properties. If a chemical potential is pure imaginary  $\mu = i\mu_I$ , then  $(z)^* = z^{-1}$  and  $(\det \Delta(\mu_I))^* = (\det(\Delta(\mu_I)))$ . These conditions bring about the first property  $c_n^* = c_{-n}$ . Note that  $c_{-N_{\text{red}}/2} = c_{N_{\text{red}}/2} = \prod_{n=1}^{N_{\text{red}}} \lambda_n = 1$ .

The second property is concerned with the center transformation  $Z_3$ . Under  $Z_3$  transformation, the time components of the link variables are transformed as

$$U_4(t_i) \rightarrow w U_4(t_i), \quad (21)$$

where  $w = \exp(2\pi i/3)$  is an element of  $Z_3$ . Regarding the  $n$ -th term in Eq. (20), if the winding number  $n$  is a multiple of  $N_c$ , the coefficient  $c_n$  is  $Z_3$  invariant, otherwise  $c_n$  is not  $Z_3$  invariant. Thus,  $c_n$  are classified in terms of  $Z_3$

$$c_n \cdots \begin{cases} \text{center invariant} & (n = 3m) \\ \text{center variant} & (n = 3m + 1, 3m + 2) \end{cases} \quad (22)$$

where  $m$  is an integer. It is known that the center symmetry is explicitly broken in the presence of quarks. In the quark determinant, the explicit breaking of the center symmetry is caused by the terms having winding numbers not multiple of  $N_c$ .

### III. NUMERICAL RESULTS

In this section, we demonstrate the calculation of the quark determinant  $\det \Delta(\mu)$  using the reduction formula. In order to see the temperature dependence of  $\det \Delta(\mu)$ , we set  $\beta = 1.85$  and  $2.0$ . We employ  $(\kappa, C_{SW}) = (0.14007, 1.5759)$  and  $(0.1369, 1.5058)$  for  $\beta = 1.85$  and  $2.0$ , respectively. We perform hybrid Monte Carlo (HMC) simulations on the  $4^4$  lattice with 1,000 quench updates and 100 full QCD HMC trajectories as thermalization. After the thermalization, we measure the quark determinant on four configurations separated by 20 HMC trajectories between measurements. Fundamental numerical data of the configurations used for the measurements are shown in Table I and II.

TABLE I: The values of the determinant with  $\mu = 0$ , Polyakov loop and plaquette for  $\beta = 1.85$ . (i), (ii), (iii) and (iv) correspond to the configurations measured.

	$\det \Delta(0)$	Polyakov loop	Plaquette
(i)	$3.0957 \times 10^{-19}$	$0.04377 - 0.25418i$	0.53338
(ii)	$2.0921 \times 10^{-21}$	$-0.03234 + 0.08711i$	0.50668
(iii)	$2.2560 \times 10^{-21}$	$-0.16365 - 0.10135i$	0.52471
(iv)	$5.1115 \times 10^{-18}$	$0.49234 - 0.12163i$	0.53313

TABLE II: The values of the determinant with  $\mu = 0$ , Polyakov loop and plaquette for  $\beta = 2.0$ .

	$\det \Delta(0)$	Polyakov loop	Plaquette
(i)	$8.7586 \times 10^{-12}$	$0.37590 + 0.0041i$	0.57810
(ii)	$3.0329 \times 10^{-12}$	$0.13827 - 0.1978i$	0.57107
(iii)	$1.1159 \times 10^{-12}$	$-0.22324 - 0.4285i$	0.57491
(iv)	$1.2578 \times 10^{-12}$	$-0.35711 - 0.6028i$	0.57954

One of the advantages of the reduction method is that it makes easy to calculate the  $\mu$  dependence of the quark determinant. Once we perform the reduction procedure and obtain  $\lambda_n$  or  $c_n$ , we can obtain  $\det \Delta(\mu)$  for arbitrary  $\mu$ . In Figs. 3 and 4, we show the  $\mu$  dependence of the determinant. The values remain near the starting points when  $\mu$  is small, and move rapidly when  $\mu$  exceeds around 0.9.

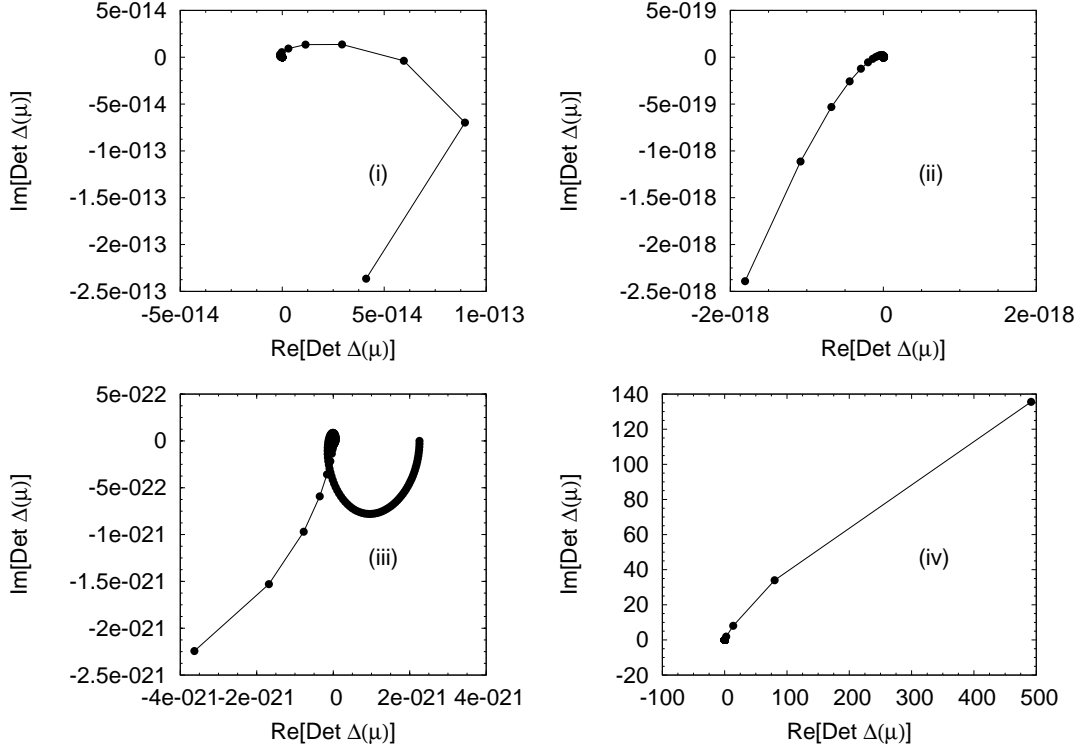


FIG. 3: Parametric plot of  $\text{Det} \Delta(\mu)$  from  $\mu = 0$  to  $\mu = 1$  for  $\beta = 1.85$ . The points are denoted for  $\delta\mu = 0.01$ .

Next, we study the reduction method in more detail. The distribution of the eigenvalues  $\lambda$  of the reduced matrix  $Q$  is shown in Figs. 5. We observe that the eigenvalues are split in two regions. Almost half of the eigenvalues are distributed in a region  $|\lambda| \gtrsim 5$ , and the other half in a region  $|\lambda| \lesssim 0.5$ . There is a margin between two regions, where no eigenvalue is found, as we can see in the right panels in Fig. 5. The splitting of the eigenvalues is observed in the eight measurements. Note that the eigenvalues are constrained by the condition  $\prod_{n=1}^{N_{\text{red}}} \lambda_n = 1$ . Qualitatively, this can be understood from the fact that the matrix  $Q$  is a product of the block matrices  $A_i = (\alpha_i^{-1} \beta_i)$ . It is expected that when the system is in equilibrium  $A_i$  moderately depends on time. In such a case, we can express  $A_i \sim \bar{A} + \delta A_i$ , where  $\bar{A}$  is independent of time. Assuming the time-dependent part  $\delta A_i$  is small,  $Q = \prod_{i=1}^{N_t} A_i \sim \bar{A}^{N_t} + \mathcal{O}(\delta)$ . Then,  $\bar{A}^{N_t}$  causes the splitting of the eigenvalues of the matrix  $Q$  for  $\text{eigen}(\bar{A}) > 1$  and  $\text{eigen}(\bar{A}) < 1$  cases.

The coefficient  $c_n$  is a polynomial of the eigenvalues  $\lambda$  according to Eq. (19). Because the number of the eigenvalues  $N_{\text{red}}$  is large, there appear two numerical problems. First problem is for an accuracy. We employ a recursive method in order to determine  $c_n$  in enough precision. Second problem is that  $c_n$  exceeds the range where a number can be represented in double precision: about  $10^{-308} \sim 10^{308}$ . In order to overcome this problem, we develop a special routine to extend exponential part. See Appendix B. For the check, we compare our results with those obtained by using FM multi-precision library (FMLIB)[23].

We plot the absolute value of  $c_n$  as a function of the winding number  $n$  in Figs. 6, where we show the results only for the configurations (i) both in high and low temperatures because results for the other configurations are



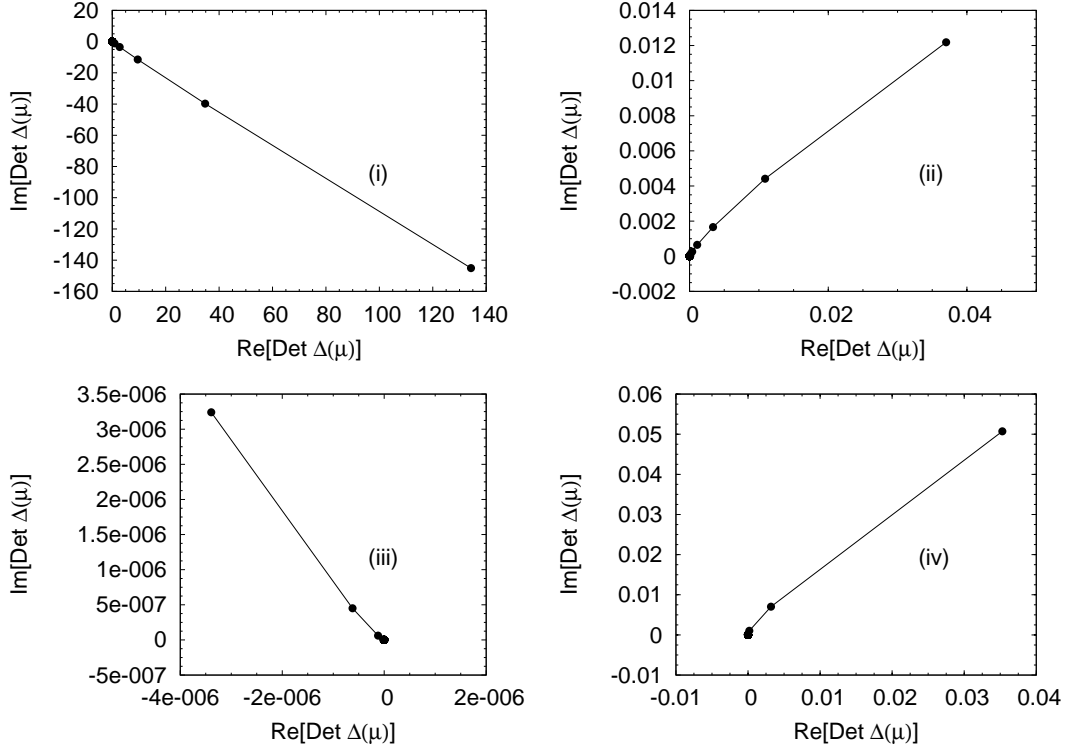


FIG. 4: Parametric plot of  $\text{Det}\Delta(\mu)$  from  $\mu = 0$  to  $\mu = 1$  for  $\beta = 2.0$ . The points are denoted for  $\delta\mu = 0.01$ .

very similar to Figs. 6. As we have mentioned,  $|c_n|$  goes over the standard numerical range and reaches at  $10^{900}$  at most, which is much larger than the maximum value in double precision. Note that the overall factor  $C$  is order  $10^{-900}$ , then the cancellation between  $C$  and  $c_n$  makes their product  $C_n = Cc_n$  ordinary order. For both  $\beta = 1.8$  and  $2.0$ , we find that  $|c_n|$  is maximum at  $n = 0$  and decreases exponentially as  $|n|$  becomes larger.

Next, we show the absolute value of  $C_n e^{n\mu/T}$  for several chemical potentials in Figs. 7 and 8. In contrast to  $|c_n|$ , the fugacity factor  $e^{n\mu/T}$  becomes larger as  $n$  becomes larger. The difference between the  $n$ -dependence of  $|c_n|$  and  $e^{n\mu/T}$  leads to a peak for  $|C_n e^{n\mu/T}|$ , as we can see in Figs. 7 and 8. Several terms in the vicinity of the peak dominate  $\det \Delta(\mu)$ . For instance,  $\det \Delta(0)$  is dominated by terms near  $n = 0$ . The location of the peak moves towards larger values of  $n$  as  $\mu$  becomes larger. However the  $\mu$  dependence of the location of the peak is not so strong. Even for the chemical potential near to  $\mu = 1$ , significant contributions come from terms with  $n < 100$ . In the following, we consider terms with  $n < 100$ .

The phase of  $c_n$  as a function of  $n$  are shown in Figs. 9 and Figs. 10. In all the eight configurations, there is a symmetry under a rotation with  $\pi$ . This symmetry indicates the relation  $c_n^* = c_{-n}$  is numerically satisfied. The phase of  $c_n$  complicatedly depends on the winding number, temperature and configuration. We find that there are two particular  $n$ -dependence. One is that the phase of  $c_n$  is a continuous function of  $n$ , e.g. see (iv) in Figs. 9. (This means that we can fit the phase of  $c_n$  in terms of a continuous function, although  $n$  is not a continuous variable.) The other is that the phase of  $c_n$  is split into three lines classified in terms of  $\text{mod}(n, 3)$ , e.g. see (i) in Figs. 9. Each line is a continuous function of  $n = 3m, 3m + 1$  or  $3m + 2$  and there is a gap about  $2\pi/3$  between lines. This

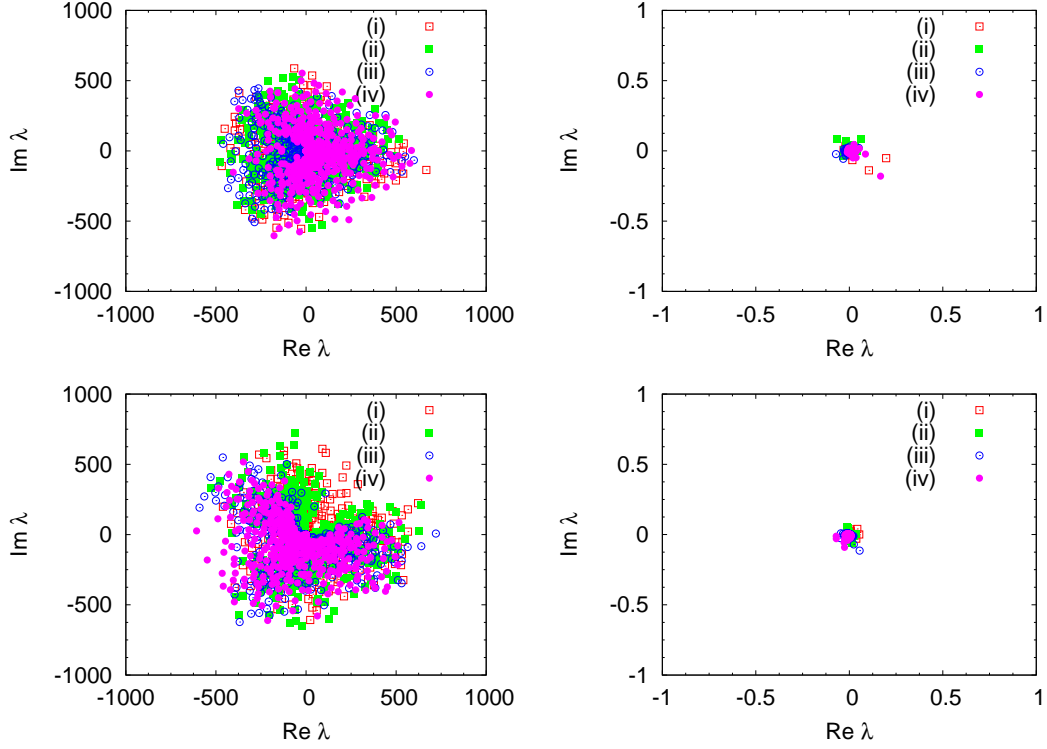


FIG. 5: The distribution of the eigenvalues  $\lambda$  in the complex plane. The topped and bottomed panels are for  $\beta = 1.85$  and  $2.0$ , respectively. The left and right panels show the distributions in two different scales.

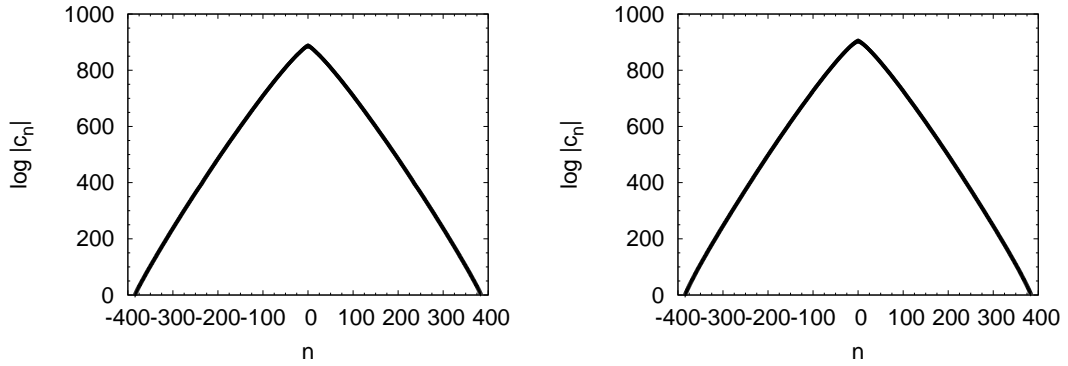


FIG. 6: The absolute values of  $c_n$  in log scale. The left and right panels are for  $\beta = 1.85$  and  $2.0$ , respectively. The results are obtained in the configurations (i).

splitting causes the cancellation of  $C_n e^{n\mu/T}$  among neighboring three terms with  $n = 3m, 3m + 1, 3m + 2$  and suppresses the magnitude of the determinant. For instance, the four values of  $\det \Delta(\mu)$  corresponding to the four configurations in  $\beta = 1.85$  are classified in two groups, as we have seen in Figs. 3;  $\det \Delta(\mu)$  is of order  $10^{-20}$  in the configurations (i), (ii) and (iii), and it is of order 100 in the configuration (iv). This observation is related to the behavior of the phase of  $c_n$ .

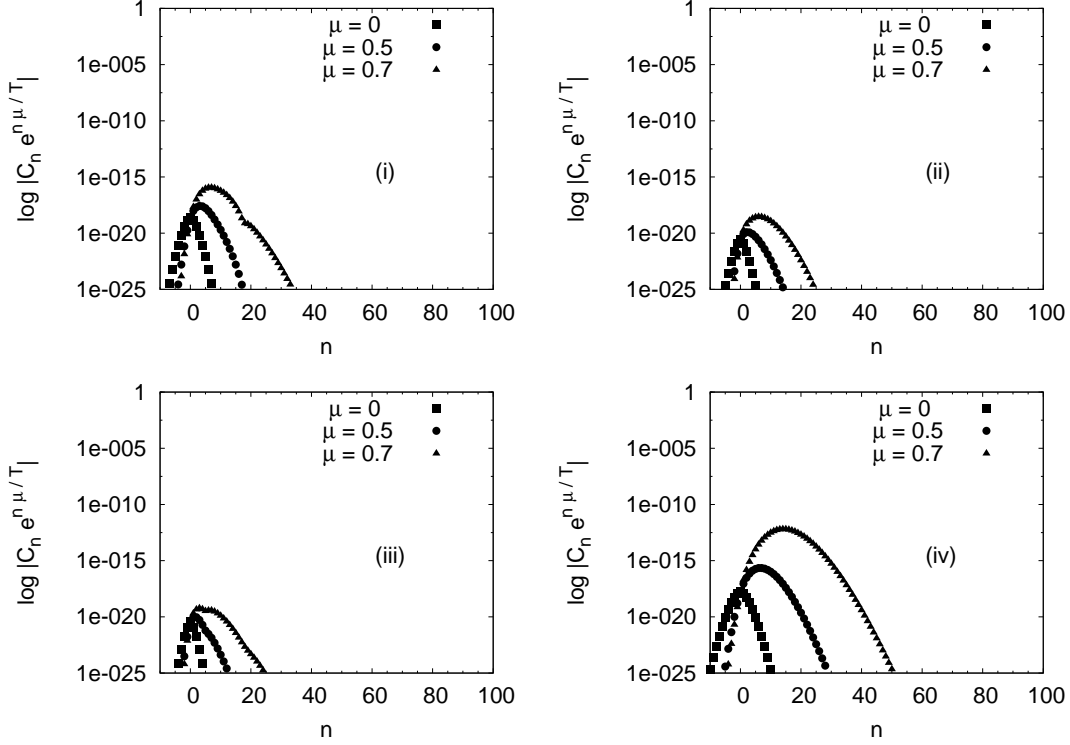


FIG. 7: The distribution of  $|C_n e^{n\mu/T}|$  for  $\beta = 1.85$ . The four panels correspond to the configurations (i), (ii), (iii) and (iv), respectively.

#### IV. SUMMARY

In this paper, we have presented the reduction formula for the Wilson fermion determinant. The formula reduces the numerical cost to evaluate the Wilson fermion determinant. The point is that the Wilson fermion matrix contains the projection operators, which enable to transform the fermion matrix so that the temporal part of the determinant can be performed analytically. Thus the Wilson fermion determinant is reduced to the determinant of the reduced matrix. Solving the eigenvalue problem for the reduced matrix, the determinant is expressed in powers of fugacity. Although the basic idea for the reduction method is similar to that for staggered fermions, a difference comes from the use of the projection operators.

We perform the numerical simulations on the  $4^4$  lattice and calculate the Wilson fermion determinant using the reduction formula. In order to determine the coefficients of the fugacity expansion in enough accuracy, we employ the recursive method and develop the special routine. Furthermore, we compare our results with those obtained by using a multi-precision library.

We discussed the properties of the eigenvalues of the reduced matrix and of the coefficients  $c_n$  of the fugacity expansion. The eigenvalues show an interesting behaviour; they are split in two regions. We find that there are two particular behaviours for the winding number dependence of the phase of the coefficients. One is that the phase of  $c_n$  is a continuous function of the winding number. The other is that the phase of  $c_n$  is split into three lines classified in terms of  $\text{mod}(n, 3)$  with the gap about  $2\pi/3$  between lines.

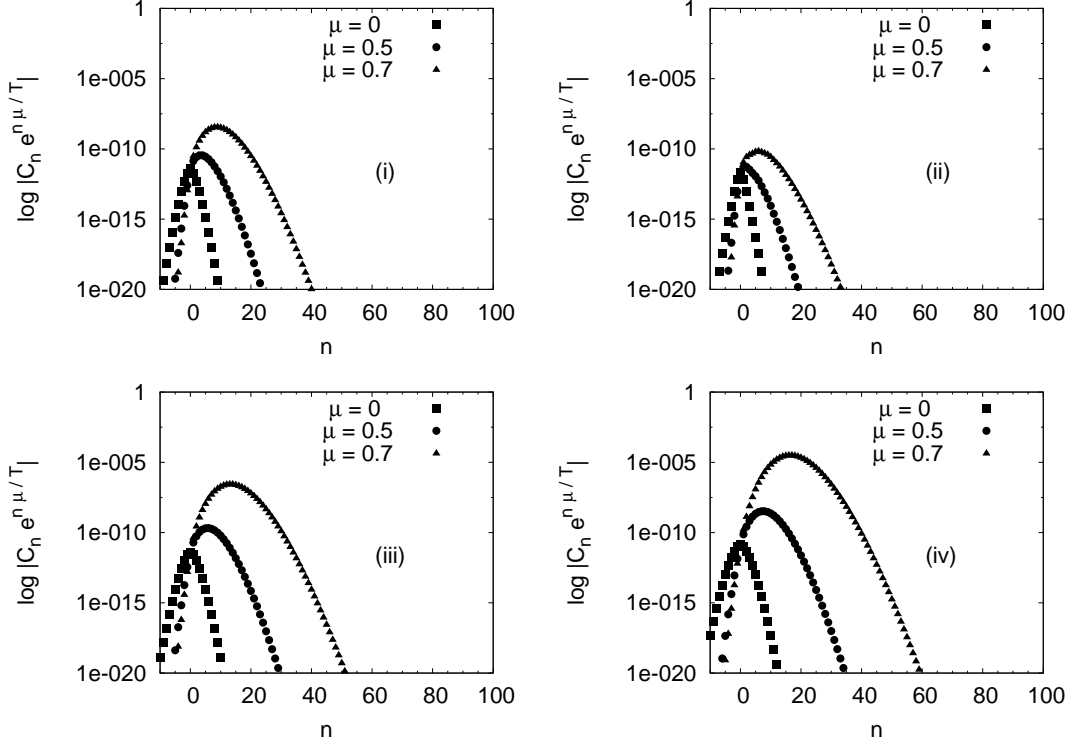


FIG. 8: The distribution of  $|C_n e^{n\mu/T}|$  for  $\beta = 2.0$ . The four panels correspond to the configurations (i), (ii), (iii) and (iv), respectively.

#### Acknowledgment

We thank Philippe de Forcrand and Andrei Alexandru for very useful discussions, without which this work could not be completed.

After finishing this work, we noticed that Urs Wenger and Andrei Alexandru have developed a similar formula for the Wilson fermions. We thank them for the correspondence.

The simulation was performed on NEC SX-8R at RCNP, and NEC SX-9 at CMC, Osaka University. We appreciate the warm hospitality and support of the RCNP administrators. This work was supported by Grants-in-Aid for Scientific Research 20340055 and 20105003.

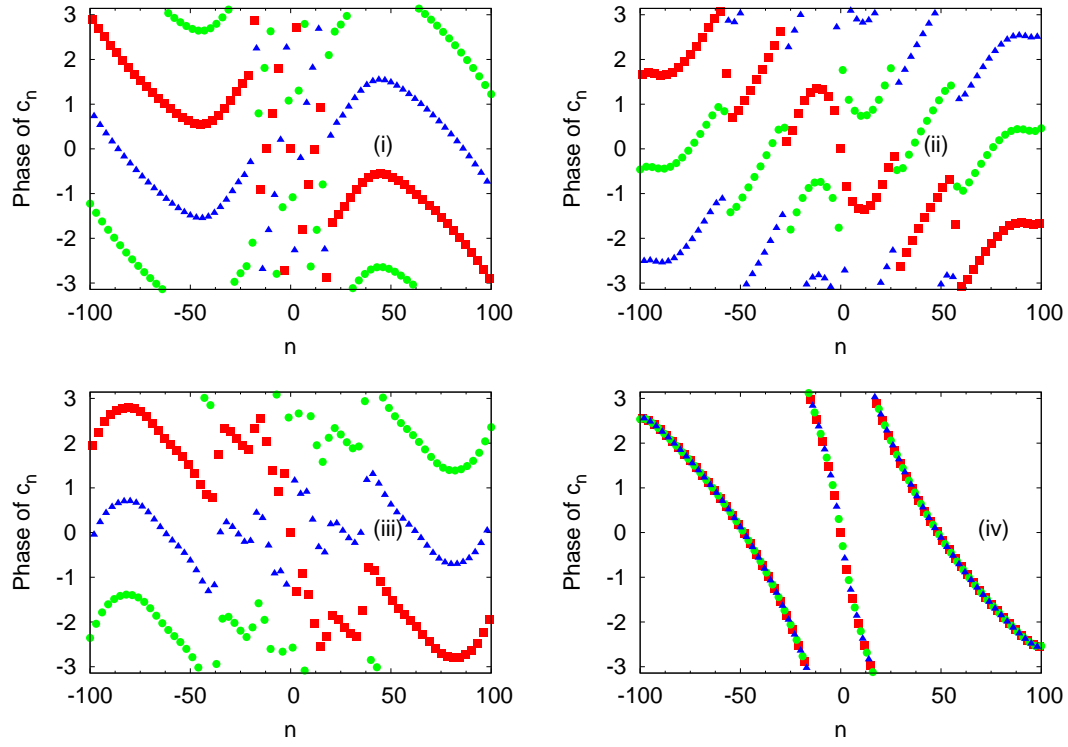


FIG. 9: The phase of  $c_n$  as functions of  $n$  for  $\beta = 1.85$ . The four panels correspond to the configurations (i), (ii), (iii) and (iv), respectively. In each panel, square, circle and triangle denote  $c_n$  for  $\text{mod}(n, 3)=0, 1$  and  $2$ , respectively.

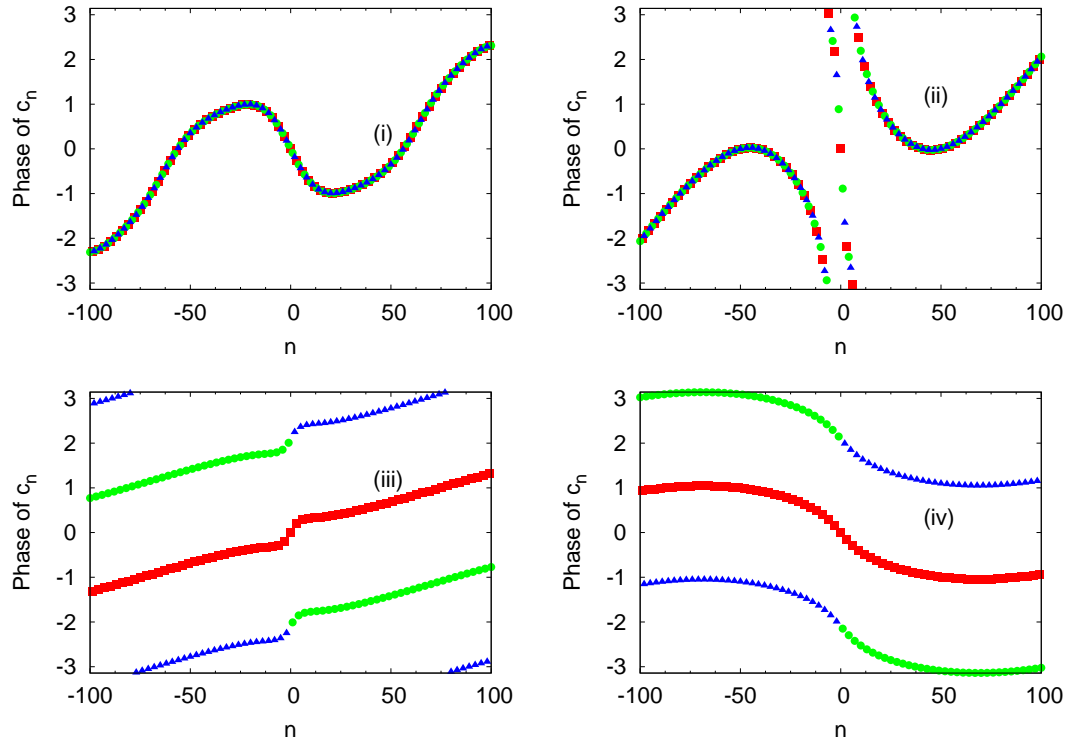


FIG. 10: The phase of  $c_n$  as functions of  $n$  for  $\beta = 2.0$ . The four panels correspond to the configurations (i), (ii), (iii) and (iv), respectively. In each panel, square, circle and triangle denote  $c_n$  for  $\text{mod}(n, 3)=0, 1$  and  $2$ , respectively.

### Appendix A: Determinant of permutation matrix

Here we calculate the determinant of the permutation matrix  $P$ . Since the projection operators are singular  $\det(r_{\pm}) = 0$ , we need to use a simple trick in order to obtain  $\det P$ ; first we reduce the determinant in the case that  $r \neq 1$ . Then we take the limit  $r \rightarrow 1$ , after eliminating the singularity. To perform this, we summarize identities of the projection operators for arbitrary  $r$ . They are defined by

$$r_{\pm} = \frac{r \pm \gamma_4}{2}. \quad (\text{A1})$$

Using the definitions, it is straightforward to obtain

$$r_+ r_- = r_- r_+ = \frac{r^2 - 1}{4} = \epsilon. \quad (\text{A2a})$$

These equations lead to the inverse matrices

$$(r_+)^{-1} = \frac{1}{\epsilon} r_- , \quad (r_-)^{-1} = \frac{1}{\epsilon} r_+. \quad (\text{A2b})$$

Using Eqs. (A2), we obtain

$$\begin{aligned} \det P &= \begin{vmatrix} c_a r_- & c_b r_+ z^{-1} V_{1,2} & & & \\ & c_a r_- & c_b r_+ z^{-1} V_{2,3} & & \\ & & c_a r_- & \ddots & \\ & & & \ddots & c_b r_+ z^{-1} V_{N_t-1, N_t} \\ -c_b r_+ z^{-1} V_{N_t, 1} & & & & c_a r_- \end{vmatrix} \\ &= \det \left( c_a^{N_t} r_-^{N_t} + c_b^{N_t} r_+^{N_t} z^{-N_t} \prod_{t_i=1}^{N_t} V_{t_i, t_i+1} \right) \end{aligned} \quad (\text{A3})$$

Considering the Dirac components,  $(r_{\pm})^{N_t}$  are given by

$$(r_+)^{N_t} = \begin{pmatrix} \left(\frac{r+1}{2}\right)^2 & & & \\ & \left(\frac{r+1}{2}\right)^2 & & \\ & & \left(\frac{r-1}{2}\right)^2 & \\ & & & \left(\frac{r-1}{2}\right)^2 \end{pmatrix}, \quad (\text{A4a})$$

$$(r_-)^{N_t} = \begin{pmatrix} \left(\frac{r-1}{2}\right)^2 & & & \\ & \left(\frac{r-1}{2}\right)^2 & & \\ & & \left(\frac{r+1}{2}\right)^2 & \\ & & & \left(\frac{r+1}{2}\right)^2 \end{pmatrix}. \quad (\text{A4b})$$

Having these two terms, there is no singularity in Eq. (A3). Then, we obtain

$$\det P = z^{-N/2} (c_a c_b)^{N/2}. \quad (\text{A5})$$

### Appendix B: Calculation of coefficients $c_n$

As we have shown, the coefficients  $c_n$  in Eq. (19) vary from order one to order  $10^{900}$  even on the small  $4^4$  lattice. They cannot be handled in the double precision. This problem usually happens when we consider expansions of the fermion determinant. So far, arbitrary accuracy libraries are often employed in order to calculate the coefficients.

We calculate  $c_n$  as follows in a recursive way:

$$\sum_{k=0}^M C'_k \xi^k = (B_0 + B_1 \xi) \sum_{k=0}^{M-1} C_k \xi^k \quad (\text{B1})$$

and

$$C'_0 = B_0 C_0 \quad (\text{B2})$$

$$C'_k = B_{k-1} C_k + B_k C_{k-1} \quad (k = 1, 2, \dots, M-1) \quad (\text{B3})$$

$$C'_M = B_1 C_{M-1} \quad (\text{B4})$$

In order to express  $C_k$ , we need wide range of floating numbers, but in Eqs. (B3) we do not need very high precision. In other words, we need wide range of the exponent, but we do not need very large significant numbers.

We express each real and imaginary parts of  $C_k$  in a form of

$$a \times b^L \quad (\text{B5})$$

where

$$1 \leq |a| < b \quad (\text{B6})$$

and  $a$  is a double precision real and  $L$  is an integer. When we solve the recursion relation Eqs. (B3), we express all  $C_k$ ,  $C'_k$  and  $B_k$  in this form. The base  $b$  can be any number, and we set it to be 8.

To see if this simple trick works or not, we calculate several cases by this method, and by a high accuracy library, FMLIB[23]. We got the same results. Although this method works for obtaining the coefficients,  $C_i$  in a sufficient double precision, we found a peculiar configuration on which a huge cancellation occurs in the sum of  $C_i \times \exp(i\mu/T)$  and the double precision is not enough to get a correct value of the determinant.

### Appendix C: Alternative approach

In this appendix, we give another possible transformation of the Wilson fermion determinant. It is more direct extension of the Gibbs's approach for the staggered fermion, and may give a general base. Unfortunately, in present-days numerical algorithms we cannot find a reliable one to solve a generalized eigenvalue problem if involved matrices are singular. But if in future this problem is solved, the following can be another good starting point.

Keeping in mind that for Wilson fermions,  $(-\kappa(r - \gamma_4)V)^{-1}$  does not exist unless the Wilson term  $r \neq 1$ , we



can apply similar transformation in the staggered fermion case by Gibbs to the Wilson fermion, and get

$$\begin{aligned}
\det \Delta &= \det \frac{1}{z} (zB + z^2(-\kappa(r + \gamma_4)V^\dagger) + (-\kappa(r - \gamma_4)V)) \\
&= \det \frac{1}{z} (zBV + z^2(-\kappa(r + \gamma_4)) + (-\kappa(r - \gamma_4)V^2)) V^{-1} \\
&= z^{-N} \left| \begin{array}{cc} -BV - z(-\kappa(r + \gamma_4)) & I \\ \kappa(r - \gamma_4)V^2 & -z \end{array} \right| / \det V \\
&= z^{-N} \left| \begin{pmatrix} -BV & I \\ \kappa(r - \gamma_4)V^2 & 0 \end{pmatrix} - z \begin{pmatrix} -\kappa(r + \gamma_4) & 0 \\ 0 & I \end{pmatrix} \right| \tag{C1}
\end{aligned}$$

Here the block-matrices are given by

$$BV = \left( \begin{array}{c|c|c|c|c} 0 & B_1 V_{12} & 0 & \cdots & 0 \\ \hline 0 & 0 & B_2 V_{23} & \cdots & 0 \\ \hline 0 & 0 & 0 & \cdots & \\ \cdots & \cdots & \cdots & \cdots & \cdots \\ \hline & & \cdots & B_{N_t-2} V_{N_t-2N_t-1} & 0 \\ \hline 0 & 0 & \cdots & 0 & B_{N_t-1} V_{N_t-1N_t} \\ \hline B_{N_t} V_{N_t1} & 0 & \cdots & 0 & 0 \end{array} \right),$$

and

$$V^2 = \left( \begin{array}{c|c|c|c|c|c} 0 & 0 & V_{12} V_{23} & 0 & \cdots & 0 \\ \hline 0 & 0 & 0 & V_{23} V_{34} & \cdots & 0 \\ \hline 0 & 0 & 0 & \cdots & & \\ \cdots & \cdots & \cdots & \cdots & \cdots & \\ \hline & & & \cdots & 0 & V_{N_t-2N_t-1} V_{N_t-1N_t} \\ \hline V_{N_t-1N_t} V_{N_t1} & 0 & & \cdots & 0 & 0 \\ \hline 0 & V_{N_t1} V_{12} & 0 & \cdots & 0 & 0 \end{array} \right).$$

By exchange columns and rows,

$$\begin{vmatrix} -BV & I \\ \kappa(r - \gamma_4)V^2 & 0 \end{vmatrix} \rightarrow \quad (C2)$$

0	0	$-B_1V_{12}$	1	$\dots$	$\dots$		0	0
0	0	$\alpha V_{N_1 1}V_{12}$	0	$\dots$	$\dots$		0	0
0	0	0	0	$-B_2V_{23}$	1	$\dots$		
0	0	0	0	$\alpha V_{12}V_{23}$	0	$\dots$		
$\dots$	$\dots$	$\dots$	$\dots$	$\dots$	$\dots$	$\dots$		
$\dots$	$\dots$	$\dots$	$\dots$	$\dots$	$\dots$	$\dots$		
$\dots$	$\dots$	$\dots$	$\dots$	$\dots$	$\dots$	$\dots$	$-B_{N_t-1}V_{N_t-1N_t}$	1
$\dots$	$\dots$	$\dots$	$\dots$	$\dots$	$\dots$	$\dots$	$\alpha V_{N_t-2N_t-1}V_{N_t-1N_t}$	0
$-B_{N_t}V_{N_t 1}$	1	0	0	$\dots$	$\dots$		0	0
$\alpha V_{N_t-1N_t}V_{N_t 1}$	0	0	0	$\dots$	$\dots$		0	0

Here we introduce  $\alpha \equiv \kappa(r - \gamma_4)$ . Applying the same exchange of the columns and rows,

$$\begin{vmatrix} -\kappa(r + \gamma_4) & 0 \\ 0 & I \end{vmatrix} \rightarrow \quad (C3)$$

$-\kappa(r + \gamma_4)$	0	0	0	$\dots$	$\dots$		0	0
0	1	0	0	$\dots$	$\dots$		0	0
0	0	$-\kappa(r + \gamma_4)$	0			$\dots$		
0	0	0	1			$\dots$		
$\dots$	$\dots$	$\dots$	$\dots$	$\dots$	$\dots$	$\dots$		
$\dots$	$\dots$	$\dots$	$\dots$	$\dots$	$\dots$	$\dots$		
0	0			$\dots$	$\dots$		$-\kappa(r + \gamma_4)$	0
0	0			$\dots$	$\dots$		0	1

Then we can write

$$\det \Delta = z^{-N} \det(T - zS) \quad (C4)$$

where

$$T = \left( \begin{array}{c|c|c|c|c} 0 & t_1 & 0 & \dots & 0 \\ \hline 0 & 0 & t_2 & \dots & 0 \\ \hline 0 & 0 & 0 & \dots & \\ \hline \dots & \dots & \dots & \dots & \dots \\ \hline & & \dots & t_{N_t-2} & 0 \\ \hline 0 & 0 & \dots & 0 & t_{N_t-1} \\ \hline t_{N_t} & 0 & \dots & 0 & 0 \end{array} \right),$$

$$t_i = \begin{pmatrix} -B_i V_{i,i+1} & 1 \\ \kappa(r - \gamma_4) V_{i-1,i} V_{i,i+1} & 0 \end{pmatrix} \quad (C5)$$

and

$$S = \left( \begin{array}{c|c|c|c|c} s & 0 & 0 & \cdots & 0 \\ \hline 0 & s & 0 & \cdots & 0 \\ \hline 0 & 0 & 0 & \cdots & \\ \hline \cdots & \cdots & \cdots & \cdots & \cdots \\ \hline 0 & 0 & & \cdots & s \\ \hline 0 & 0 & & \cdots & 0 \end{array} \right) .$$

$$s = \begin{pmatrix} -\kappa(r + \gamma_4) & 0 \\ 0 & I \end{pmatrix} . \quad (\text{C6})$$

Each  $t_i$  and  $s$  is  $(4N_c N_x N_y N_z) \times (4N_c N_x N_y N_z)$  matrix.

Eq. (C4) is a form of the generalized eigenvalue problem[24]. There is a mathematical theorem (Generalized Schur Decomposition) which tells us that there exist unitary matrices  $Y$  and  $Z$  such that  $Y^\dagger S Z$  and  $Y^\dagger T Z$  are upper triangular. Let  $\alpha_k$  and  $\beta_k$  be diagonal elements of these matrices. Then

$$\det(T - zS) = \det Y Z^\dagger \prod_k (\alpha_k - z\beta_k) \quad (\text{C7})$$

Half of  $\alpha$ 's and  $\beta$ 's vanish.

This formula has an advantage that  $T$  and  $S$  do not have inverse matrix like  $Q$  in Eq. (17), and can be easily constructed. A problem is that matrices  $T$  and  $S$  are singular. To our knowledge, no stable algorithm is know to solve the generalized eigenvalue problem in such a case.

- 
- [1] A. Andronic et al., arXiv:0911.4806.
  - [2] Z. Fodor, S. D. Katz, JHEP, 0203 (2002) 014, (hep-lat/0106002). Phys. Lett. B534 (2002) 87, (hep-lat/0104001)
  - [3] M. D'Elia, M. P. Lombardo, Proceedings of the GISELDA Meeting held in Frascati, Italy, 14-18 January 2002, hep-lat/0205022.
  - [4] Ph. de Forcrand, O. Philipsen, Nucl. Phys. **B642** 290 (2002), hep-lat/0205016.
  - [5] D. E. Miller and K. Redlich, Phys. Rev. D35, (1987) 2524-2530.
  - [6] J. Engels, O. Kaczmarek, F. Karsch and E. Laermann, Nucl.Phys. B558 (1999) 307-326, hep-lat/9903030;
  - [7] A. Gocksch, Phys. Rev. Lett. 61 (1988) 2054.
  - [8] P.E. Gibbs, Phys. Lett., B172 (1986) 53.
  - [9] A. Hasenfratz and D. Toussaint, D, Nucl. Phys. **B 371**, 539 (1992).
  - [10] S. Kratochvila and P. de Forcrand, Nucl. Phys. Proc. Suppl. **140**, 514 (2005), [hep-lat/0409072].
  - [11] S. Kratochvila and P. de Forcrand, PoS **LAT2005**, 167 (2006), [hep-lat/0509143].
  - [12] P. de Forcrand and S. Kratochvila, Nucl. Phys. Proc. Suppl. **153**, 62 (2006), [hep-lat/0602024].
  - [13] S. Kratochvila and P. de Forcrand, Phys. Rev. **D73**, 114512 (2006), [hep-lat/0602005].
  - [14] A. Alexandru, M. Faber, I. Horvath and K.-F. Liu, Phys. Rev. **D72**, 114513 (2005), [hep-lat/0507020].
  - [15] A. Alexandru, A. Li and K.-F. Liu, PoS **LAT2007**, 167 (2007), [arXiv:0711.2678].
  - [16] A. Li, A. Alexandru and K.-F. Liu, PoS **LAT2007**, 203 (2007), [arXiv:0711.2692].
  - [17] A. Li, X. Meng, A. Alexandru and K.-F. Liu, PoS **LATTICE2008**, 178 (2008), [arXiv:0810.2349].

- [18] X.-f. Meng, A. Li, A. Alexandru and K.-F. Liu, PoS **LATTICE2008**, 032 (2008), [arXiv:0811.2112].
- [19] J. Danzer and C. Gattringer, Phys. Rev. **D78**, 114506 (2008), [arXiv:0809.2736].
- [20] C. Gattringer and L. Liptak, arXiv:0906.1088.
- [21] J. Danzer, C. Gattringer and L. Liptak, PoS **LAT2009**, 185 (2009), [arXiv:0910.3541].
- [22] A. Borici, Prog.Theor.Phys.Suppl.153:335-339,2004.
- [23] <http://myweb.lmu.edu/dmsmith/fmllib.html>
- [24] G. H. Golub and C. F. Van Loan, “Matrix Computations”, John Hopkins Univ. Press, 1996.